Clinical Radiology 74 (2019) 797–804

Contents lists available at ScienceDirect

Clinical Radiology

journal homepage: www.clinicalradiologyonline.net

Differentiation of hepatocellular carcinoma from non-hepatocellular malignant tumours of liver by chemical-shift MRI at 3 T☆

K. Ozturk [a,*,1], E. Soylu [a], Z. Yazici [a], G. Ozkaya [b], G. Savci [a,1]

[a] Department of Radiology, Uludag University Faculty of Medicine, Gorukle Street, Bursa, Turkey
[b] Department of Biostatistics, Uludag University Faculty of Medicine, Gorukle Street, Bursa, Turkey

ARTICLE INFORMATION

Article history:
Received 9 April 2019
Accepted 12 June 2019

AIM: To evaluate the diagnostic performance of chemical shift magnetic resonance imaging (MRI) in distinguishing hepatocellular carcinomas (HCCs) from non-hepatocellular malignant tumours (non-HCCs) of the liver.

MATERIALS AND METHODS: Patients with a diagnosis of malignant liver tumours examined at 3 T MRI were included in this retrospective study. Forty-seven HCCs and 75 non-HCCs that were studied with chemical-shift MRI between January 2012 and October 2016 were retrieved from the radiology database. Two blinded observers measured the signal intensities of the tumours, adjacent normal-looking liver parenchyma, and spleen on chemical-shift MRI. The fat quantification for HCCs, non-HCCs, and adjacent normal-looking liver parenchyma were calculated by using the spleen as a reference standard. The subtraction scores were calculated by subtracting fat percentages in liver parenchyma from those in tumours. The sensitivity, specificity, positive predictive value (PPV), and negative predictive value (NPV) of the fat percentage subtraction scores in distinguishing HCCs from non-HCCs were calculated.

RESULTS: According to the optimal cut-off value acquired from both readers, a subtraction score >-0.26 was considered to be a HCC. Fat signal percentage subtraction scores were ≥-0.26 in 45 of 47 HCCs and were <-0.26 in 69 of 75 non-HCCs. The sensitivity, specificity, PPV, and NPV of fat signal percentage subtraction score to differentiate HCCs from non-HCCs were found to be 95.7%, 89.3%, 84.9%, and 97.1%, respectively.

CONCLUSION: Intracytoplasmic lipid in HCCs demonstrated by quantitative chemical-shift MRI may be a potentially powerful imaging biomarker to distinguish HCCs from the other malignant liver tumours.

Introduction

The liver hosts many types of benign or malignant tumours. Hepatocellular carcinoma (HCC) is the most common primary liver malignancy and the third most common cause of cancer-related deaths worldwide.[1] The liver is one of the most common sites of haematogenous metastasis; 25% of all solid-organ metastases could be seen in the liver.[2]

☆ Preliminary results of this study was presented as an oral presentation at the European Congress of Radiology (ECR) 2016 Annual Meeting, 2–6 March 2016, Vienna, Austria.

* Guarantor and correspondent: K. Ozturk, Department of Radiology, Uludag University Faculty of Medicine, Gorukle Street, Nilufer, Bursa, 16059, Turkey. Tel.: +90 224 2953341.

E-mail address: keremozturk@uludag.edu.tr (K. Ozturk).

[1] These authors contributed equally as co-senior authors of this manuscript.

https://doi.org/10.1016/j.crad.2019.06.006
0009-9260/

It is also a well-known entity that dysplastic nodules in patients with cirrhosis may demonstrate malignant transformation to HCC.[3,4] It is important to differentiate HCCs from the non-hepatocellular malignant tumours (non-HCCs) of the liver as treatment options for HCCs are different from non-HCCs.

Magnetic resonance imaging (MRI) is a comprehensive radiological technique providing detailed information on liver tumours; however, differentiation of HCCs from other malignant liver tumours, including metastases, may not always be possible with conventional MRI techniques; sometimes, more advanced techniques or even histopathological evaluation may be necessary.[5] This is especially problematic in patients with liver metastasis of unknown primary tumours.

HCCs may contain intratumoural fat.[6] Furthermore, in cirrhotic livers, the presence of fat within a lesion may be accepted as a significant marker of malignant transformation to HCC.[7] Recently, intratumoural fat deposition more than the adjacent liver was implemented into the Liver Imaging-Reporting and Data System (LI-RADS) as an ancillary feature that favours HCC in particular.[8,9] Chemical-shift MRI, as one of the specialised imaging techniques, is a sensitive method to detect relatively small amounts of intracellular fat. The ability of this technique to detect intralesional fat increases directly with increasing magnetic field strength of an MRI system.[10]

Previous studies using the chemical-shift MRI to assess fatty changes in HCCs were mostly performed with qualitative analysis.[11] There is only one study in the literature using quantitative analysis to estimate the percentage of intracellular fat in HCCs using chemical shift imaging, in which a 1 T MRI system was used.[12] Despite the promising role of the chemical-shift MRI in the differentiation of HCCs from non-HCCs, the diagnostic value of intratumoural fatty change has not been determined. Therefore, the aim of the present study was to investigate the value of chemical-shift imaging using quantitative analysis and a 3 T MRI system in the differentiation of HCCs from non-HCCs.

Material and methods

Patients

The institutional review board approved this retrospectively designed study and waived the requirement for obtaining informed consent. The patients with either primary or metastatic malignant liver tumours examined with a 3 T MRI were included in the study. A total of 128 patients with malignant liver lesions were retrieved from the radiology database from January 2012 to October 2016. Patients having indistinct tumour margins due to motion artefacts (n=4), cystic lesions without an obvious solid component (n=1), and masses <1 cm (n=1) to avoid partial volume effect were excluded. The forty-seven HCCs and 75 non-HCCs in a total of 122 patients (50 women and 72 men; mean age, 60.4 years; age range 30–87 years) were included in the study (Table 1). For patients with multiple liver masses (n=65), only the largest tumour was evaluated to obviate sampling bias.

The diagnosis of HCC was based on the histopathological examination in 24 patients and the appropriate imaging characteristics according to the criteria in the guidelines of the American Association for the Study of Liver Diseases (AASLD)[13] in 23 patients. The final diagnosis of non-HCC was obtained by histopathological examination of the primary tumours in 39 patients and the liver metastasis in 36 patients (Table 2).

MRI technique

Images were acquired using a 3 T MRI system (Achieva, Philips, Amsterdam, The Netherlands) by using a phased-array body coil. The sequence parameters for conventional images were as follows: T1-weighted breath-hold spoiled gradient-echo sequence (repetition time [TR]=1,625–1,787 ms, echo time [TE]=70 ms, four separate breath-holds, 17 seconds each, and matrix=320×255, flip angle=90°, number of slices=38–44, section thickness=7 mm, gap=5 mm, field of view [FOV]=36–40 cm), T2-weighted breath-hold sequence (TR=1,625–1,787 ms, TE=70 ms, four separate breath-holds, 17 seconds each, and matrix=320×255, flip angle=90°, number of slices=38–44, section thickness=7 mm, gap=5 mm, FOV=36–40 cm). After intravenous bolus injection of gadoterate meglumine (Gd-DOTA, DOTAREM, Guerbet, Roissy CdG Cedex, France) at a dose of 0.1 ml/kg, six phase arterial images were obtained using a time-determined, real-time MRI fluoroscopic technique (TR=2.8 ms, TE=1.4 ms, flip angle=10°, matrix size=192×192, 100 slices per phase, slice thickness=4 mm, gap=2 mm, FOV=40 cm).

Double-echo chemical shift phase-selective gradient-echo technique was performed using a three-dimensional (3D) fast field echo (FFE) gradient-echo breath-hold technique (TR=3.3 ms, TE=1.15–2.3 ms; flip angle=100°; matrix size=192×256; FOV=37×35 cm; voxel size=1.5×1.7×1.5 mm).

Quantitative analysis

Chemical-shift MRI images of the patients were analysed on a workstation (Easy Vision, Philips Medical Systems, Best, The Netherlands) by two radiologists who were blinded to the final diagnosis of the tumours and to each other's results. Quantitative assessment was performed by obtaining region-of-interest (ROI) measurements of the signal intensities (SIs) of hepatic tumours, adjacent normal-looking liver

Table 1
Demographic characteristics of the patients.

	HCC group	Non-HCC group
Number	47	75
Gender		
Male	37	38
Female	10	37
Age, mean (SD), years	61.7 (11.2)	59.5 (11.8)

SD, standard deviation; HCC, hepatocellular carcinoma.

Table 2
The final diagnosis of tumours was confirmed by histopathological examination in 99 patients.

Histopathological diagnosis	Biopsy site	
	Primary tumour	Metastatic tumour
Hepatocellular carcinoma	24	0
Breast tumour (adenocarcinoma)	7	10
Colorectal tumour (adenocarcinoma)	11	7
Cholangiocellular carcinoma	0	4
Stomach tumour (adenocarcinoma)	2	3
Pancreas tumour (adenocarcinoma)	6	3
Lung tumour (squamous cell carcinoma)	2	2
Neuroendocrine tumour	3	2
Leiomyosarcoma	0	2
Phaeochromocytoma	0	2
Lung tumour (small cell carcinoma)	1	1
Lymphoma	2	0
Bladder tumour (transitional cell carcinoma)	2	0
Malignant melanoma	1	0
Oesophagus tumour (adenocarcinoma)	1	0
Total	63	36

parenchyma, and spleen. Three measurements were performed on each phase of imaging. Special attention was given to using uniform ROIs of at least 1 cm in diameter, and excluding cystic, haemorrhagic, or necrotic regions. When calcification was identified in either region on CT scan if available, the calcified portions were also avoided to be included within the ROIs. SIs of the hepatic masses, liver parenchyma, and spleen were measured on the same section if possible. Spleen, which is known to be immune to fatty degeneration, was used as the internal reference standard.

The fat signal percentages were calculated using the following formulas for tumours and adjacent normal looking liver parenchyma, respectively:[14,15]

Tumour fat percentage=[(tumour SI $_{\text{in-phase}}$/spleen SI $_{\text{in-phase}}$)−(tumour SI $_{\text{opposed-phase}}$/spleen SI $_{\text{opposed-phase}}$)] × 100/[(tumour SI $_{\text{in-phase}}$/spleen SI $_{\text{in-phase}}$) × 2].

Liver parenchyma fat percentage=[(liver parenchyma SI $_{\text{in-phase}}$/spleen SI $_{\text{in-phase}}$)−(liver parenchyma SI $_{\text{opposed-phase}}$/spleen SI $_{\text{opposed-phase}}$)] × 100/[(liver parenchyma SI $_{\text{in-phase}}$/spleen SI $_{\text{in-phase}}$) × 2].

The subtraction scores were calculated as follows:

The fat percentage subtraction score=(Tumour fat percentage)−(Liver parenchyma fat percentage)

Statistical analysis

All statistical comparisons between the HCC and non-HCC groups were performed by using software of Statistical Package for the Social Sciences (SPSS, version 23.0; SPSS, Chicago, IL, USA). Receiver operating characteristic (ROC) analysis was performed using MedCalc software (MedCalc for Windows; Ostend, Belgium). Descriptive statistics were given as mean ± standard deviation or median (minimum–maximum) for continuous variables and count and percentage for categorical variables. Distribution of gender was compared between the HCC and non-HCC groups by using the Pearson chi-square test, and the Student *t*-test was used to compare the patients' ages. The mean fat percentage values were compared with the Mann–Whitney *U*-test. The ROC analysis was utilised to assess the diagnostic performance of these parameters. The optimal cut-off values were extracted from ROC analysis, which demonstrated the best differentiation scores (minimal false-negative and false-positive results) between the two groups. The sensitivity, specificity, positive predictive value (PPV), and negative predictive value (NPV) of the subtraction score in distinguishing HCC from other malignant liver tumours were calculated.

The inter-reader agreement was assessed using Cohen's k statistics. The null hypothesis of no agreement between the two readers was tested, and the associated *p*-values were calculated. A *p*-value of <0.05 was considered a statistically significant difference.

Results

The mean age of patients was 61.77±11.27 years (range, 37–85 years) in the HCC group and 59.53±11.84 years (range, 30–87 years) in the non-HCC group. There was no significant difference between the groups in terms of age ($p=0.304$). However, the groups were significantly different from each other in gender (female patients, 21.3% in HCC and 49.3% in non-HCC group; $p=0.002$; Table 1).

The median diameter of the tumours was 3.1 cm (mean, 5.3 cm; range, 1.3–12.5 cm) for the HCCs, 2.3 cm (mean, 4.5 cm; range, 2.8–13.5 cm) for the non-HCCs. There was no significant tumour size difference between the groups ($p=0.061$).

The median fat percentage values of the liver masses were 5.11 (range, −22.51 to 32.63; mean, 6.28±11.13) in the HCC group and −3.89 (range, −17.66 to 18.62; mean, −2.55±6.54) in the non-HCC group (Fig 1). There was a statistically significant fat percentage difference between the groups of tumours ($p<0.001$).

The median fat percentage subtraction score was 6.55 (range, −13.96 to 49.12; mean, 9.17±11.14) in the HCC group (Fig 2) and −5.09 (range, −46.59 to 20.79; mean, −7.54±11.45) in the non-HCC group (Fig 3); which was significantly different between the two groups ($p<0.001$; Fig 1). The fat percentage subtraction values in HCC group did not show any correlation with tumour size ($r=-0.070$; $p=0.627$).

The area under the ROC curve for differentiation of HCCs from non-HCCs was 0.737 (95% confidence interval: 0.668, 0.786) according to the fat percentage values of the liver masses and 0.936 (95% confidence interval: 0.876, 0.972) according to the fat percentage subtraction scores. The subtraction score and the fat percentage score of the liver masses were statistically different according to the pairwise comparison of the ROC curves ($p=0.002$). According to the acquired optimal cut-off value, a tumour having a fat percentage value >1.72 or a subtraction score >-0.26 was considered to be a HCC (Fig 4).

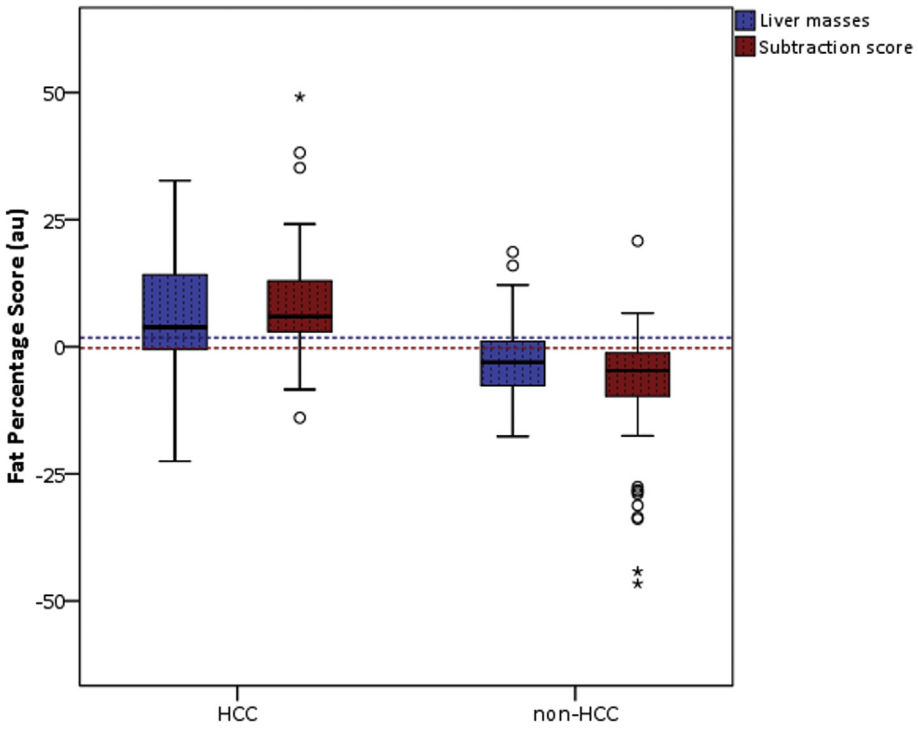

Figure 1 The box plot shows the mean fat percentage score of the liver tumours and fat percentage subtraction scores. (HCC, hepatocellular carcinoma; Error bars represent ±SD). According to the acquired optimal cut-off value, a tumour having a fat percentage score of the mass greater than 1.72 (blue dashed line) or a subtraction score >−0.26 (red dashed line) was considered to be a HCC.

When the determined cut-off value of the subtraction score was used, 45 out of 47 HCCs were correctly diagnosed as HCC (true positive result), and 69 out of 75 non-HCCs were correctly diagnosed as non-HCC (true negative result). For the fat percentage subtraction score cut-off value of −0.26 for the differentiation of HCC from non-HCCs, the sensitivity, specificity, PPV, and NPV were 95.74%, 89.33%, 84.9%, and 97.1%, respectively.

Two HCCs did not have intratumoural fat, which misled to the diagnosis of non-HCC (false-negative result), and six metastases had intratumoural fat leading to a diagnosis of HCC (false-positive result). Both false-negative HCCs were found to have T1 hyperintense appearance without signal loss on fat suppression, which was speculated to relate to the presence of intratumoural haemorrhage, copper or iron deposits.[16] Two of false-positive non-HCCs were associated

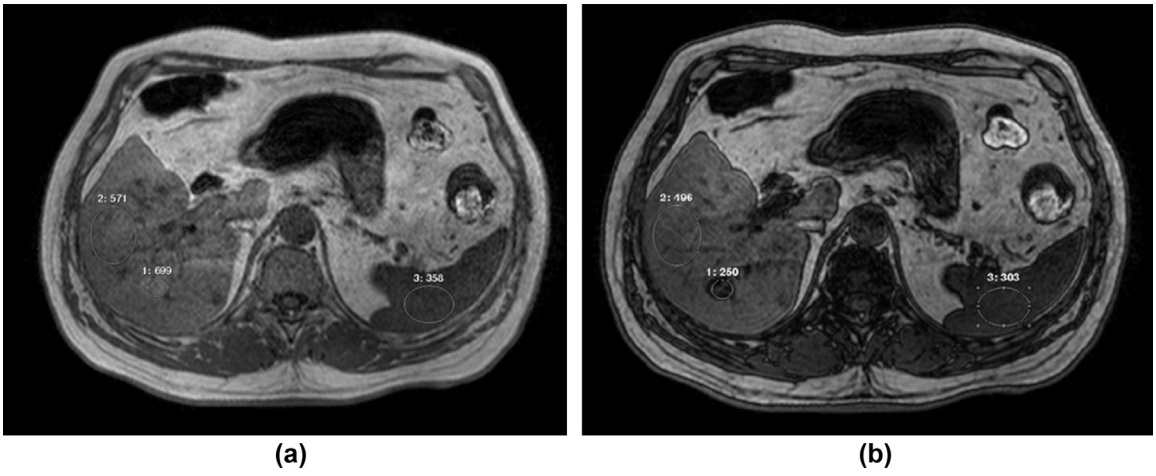

Figure 2 Dual-echo chemical-shift MRI of the pathologically proven HCC. (a) In-phase MRI image showed a tumour-to-splenic SI ratio and hepatic parenchyma-to-splenic SI ratio of 1.59. (b) Out-of-phase MRI image showed a tumour-to-splenic SI ratio and hepatic parenchyma-to-splenic SI ratio of 0.82 and 1.34, respectively. Calculated by using the Dixon method, the percentage of tumour fat was 9.2% and the percentage of liver parenchyma fat was −31%. The fat percentage subtraction score of 40.2 was consistent with HCC.

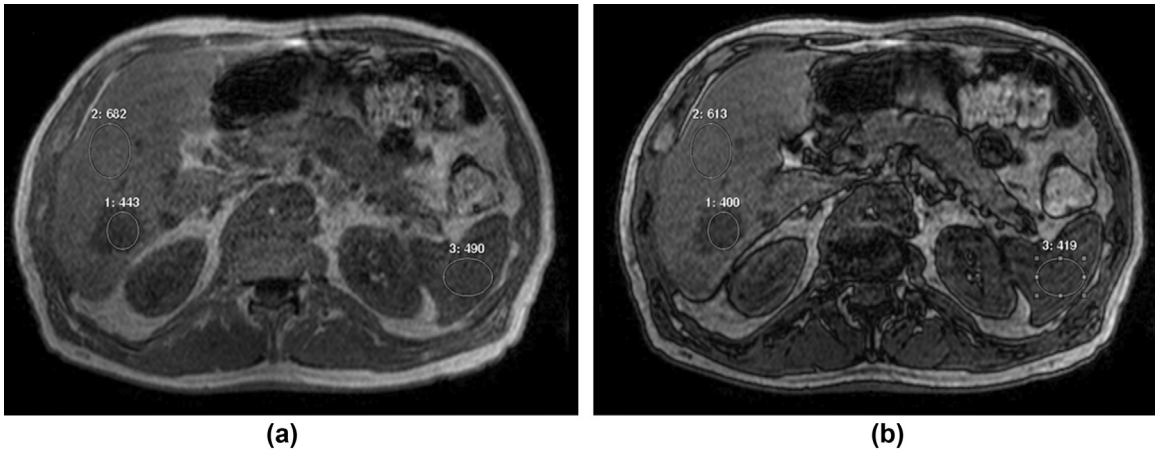

Figure 3 Dual-echo chemical-shift MRI with in-phase (a) and out-of-phase (b) images of the pathologically proven metastatic liver tumour of colon cancer. Calculated by using the Dixon method, the percentage of tumour fat was −27% and the percentage of liver parenchyma fat was −26%. The fat percentage subtraction score of −1 was consistent with non-HCC.

with liver iron overload (Fig 5). Diagnosis of parenchymal iron overload was made by using the SI differences of the in-phase and out-of-phase images, in which liver SI of the in-phase images is lower than that of the out-of-phase images.[17] Inter-reader agreement was high with an intraclass correlation coefficient of 0.858 (95% confidence interval, 0.802–0.898).

The fat percentage subtraction score in the HCC group (median, 17.05 au; range, 15.8–24.72) was significantly higher than non-HCCs (median, −17.34 au; range, −46.59 to 4.56) in patients with significant fatty liver degeneration. When 19 patients with significant fatty liver degeneration were excluded, the median fat percentage subtraction scores were found to be 6.21 (range, −13.96 to 49.12; mean, 9.33±11.48) in the HCC group and −2.19 (range, −14.13 to 20.79; mean, −3.10±5.49) in the non-HCC group; which was also significantly different between the two groups ($p<0.001$).

Discussion

HCC is a very common tumour seen worldwide with a poor prognosis.[18] It usually develops during the course of chronic liver diseases such as viral infections, chronic alcohol consumption and exposure to many kinds of toxins.[19] Development of HCC is a multistep process beginning in a hyperplastic nodule evolving to the dysplastic nodules and finally to the overt HCC.[20] Differently from most other cancers, the diagnosis of HCC can be established non-invasively using imaging without confirmatory biopsy.[21] Some MRI features, such as pseudocapsule, T1 hyperintensity, mosaic appearance, nodule-in-nodule appearance, arterial hyperenhancement, delayed washout, vascular invasion, and apparent diffusion coefficient (ADC) value may have diagnostic value for HCCs.[22] Although the individual features are non-specific for HCC, their combination is highly specific, particularly in patients with cirrhosis or other risk factors for HCC.

Intratumoural fatty metamorphosis is one of the histopathological characteristics of HCC.[23] Several studies showed that lipogenic enzymes are markedly induced in HCCs compared with background hepatic tissue and increased lipogenesis is a general molecular event in hepatocarcinogenesis.[24,25] Calvisi *et al.*[26] revealed that de-novo lipogenesis has a prognostic significance for HCC and inhibitor molecules of lipogenic signalling, including those that inhibit de-novo lipogenesis, might be useful in treatment. In human liver samples, de-novo lipogenesis was shown to be progressively induced from non-tumoural liver tissue toward the HCC. Importantly, no significant

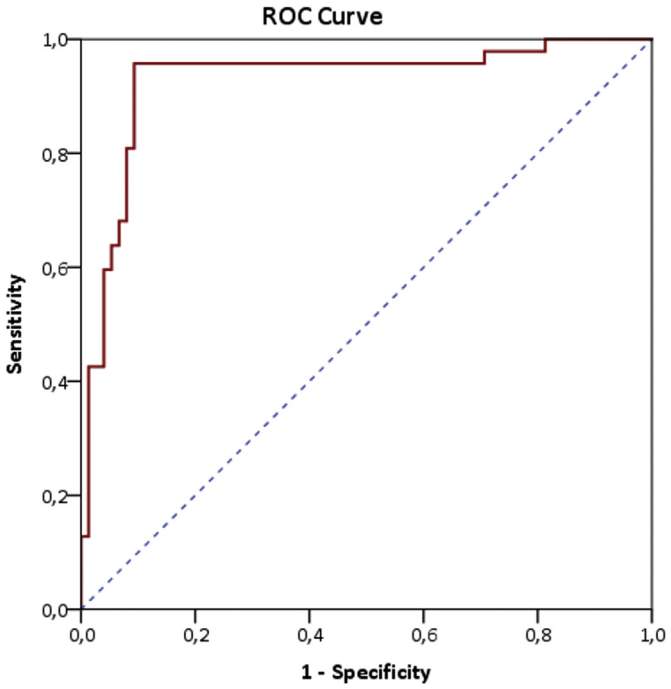

Figure 4 ROC curve for differentiation of the HCCs from non-HCCs according to the fat percentage subtraction score.

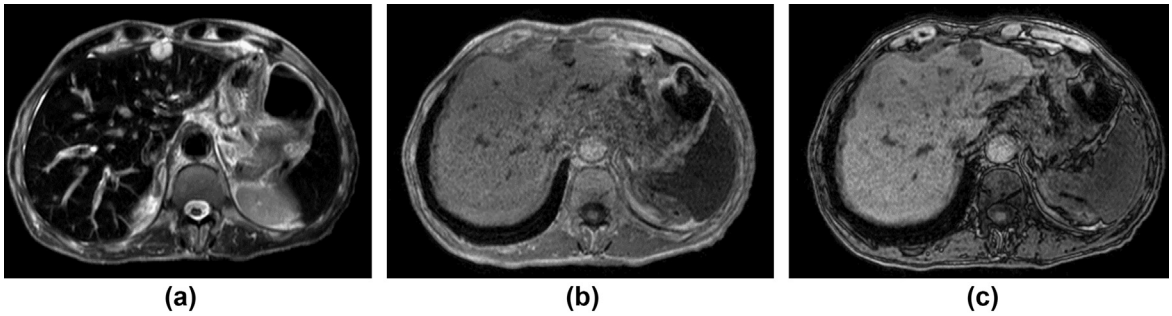

Figure 5 Imaging features of liver iron deposition on T2-weighted imaging (a), in-phase (b) and out-of-phase (c) chemical-shift MRI in a patient with liver mass and a history of haemochromatosis.

differences were detected in the extent of de-novo lipogenesis with regard to HCC aetiology, suggesting that exacerbated lipogenesis might be a general molecular phenomenon in hepatocarcinogenesis.[27] Björnsen *et al.*[28] demonstrated that fatty acid synthesis within HCCs is linked to tumour growth and proliferation.

Ultrasonography, computed tomography, and conventional MRI sequences have limited sensitivity in the detection of fat within HCCs.[29–32] Chemical-shift MRI as a non-invasive method is generally used to assess hepatic steatosis in routine practice.[30] There are few studies in the literature analysing the intratumoural fat of HCCs with chemical-shift MRI[6,12,23,32]; however, most of them used qualitative methods to determine intratumoural fat content.[6,23,32] Asayama *et al.*[23] analysed 136 HCCs using 1.5 or 3 T MRI systems and detected intratumoural fat qualitatively in 54 out of 136 patients (40%), which was also confirmed histopathologically. In another study by Min *et al.*,[32] 365 HCCs were examined using a 3 T MRI system. Sixty-six of these tumours were classified as a fat-containing HCC according to the qualitative method. On histopathology, all were proven to have fat and their fat component ranged from 10 to 95%. Additionally, two out of 229 non-fat-containing HCCs were found to have a minimal fat component on histopathological examination (<2%). The ratio of fat-containing HCCs was 18.6% in their study.

There is only one study in the literature which used a quantitative method to assess the fatty metamorphosis of HCCs on chemical-shift MRI.[12] They performed MRI of patients using a 1 T MRI system and used spleen as a reference organ. According to the percentage variation in the SI of lesions between in-phase and opposed-phase images, intratumoural lipid content was detected in 10 (14.5%) of 69 HCCs, which also confirmed by fine-needle aspiration cytology with 100% sensitivity, 100% specificity, and 100% overall accuracy.

In the present study, intratumoural fat was detected in 45 (95.7%) of 47 HCCs. For the chosen fat percentage subtraction score cut-off value of −0.26, the sensitivity, specificity, PPV, and NPV of the present method to discriminate HCCs from non-HCCs were 95.7%, 89.3%, 84.9%, and 97.1%, respectively. These results are significantly better than other reported series. The reason for this difference may be due to using a 3 T MRI system and quantitative analysis. Proton chemical-shift MRI at higher field strength has the benefit of increased signal-to-noise ratio and improved spectral separation. In addition, using a quantitative method that takes account of the intensity values of the hepatic parenchyma surrounding the tumour might be another contributory factor. The light microscopy evaluation in some radiological studies has been accepted as the reference standard for the detection of intratumoural fat content.[31,33] Interestingly, lipid detection in HCCs was reported to be as high as 42% in these studies[33]; however, in the present series, intratumoural fat was detected in most HCCs. This difference may be due to the fact that the histopathological examination may have a sampling bias. Because intracytoplasmic lipid estimation in the histological specimen is mainly based on two-dimensional measurements, MRI-based calculation of the lipid content may better reflect the actual lipid content of the tissues due to three-dimensional voxel evaluation.[34] In addition, it is speculated that there may be some sampling variability for the biopsies. By histopathological examination, only a small fraction of the tumour might be evaluated, and this could be problematic due to heterogeneous lipid distribution in the sampled tissue. The dual-echo chemical-shift MRI may better reflect *in vivo* tissue lipid fraction than traditional histopathological analysis as shown in the literature. Fischer *et al.*[35] founded a significantly higher correlation between tissue lipid fraction estimates derived from dual-echo chemical-shift MRI and the computer-based histological result compared to the traditional histopathological method of a cell-count fraction, reflecting the high inter-observer variability of visual (cell-count fraction) histopathological estimation. Dual-echo chemical-shift MRI revealed the highest accuracy and the smallest measurement bias for the quantification of tissue lipid fraction, especially for clinically relevant low lipid fraction (5%) values. Their results showed that MRI-derived fat-fraction measurements could be highly reproducible and might better reflect the "true" tissue lipid fraction in contrast to visual histopathological analysis.

According to LI-RADS, intralesional fat in higher concentration than in the adjacent hepatic parenchyma is an ancillary imaging feature favouring malignancy, HCC in particular.[36] In fact, this feature is considered to be non-contributory for the imaging-based diagnosis of HCC, in part, because the presence of fat coincided with other more

discriminatory imaging features[37]; however, the present results show that intralesional fat may be more discriminatory for HCCs than non-HCCs.

In the present series, two HCCs resulted in false-negative and six non-HCCs resulted in false-positive results according to the presence of intratumoural fat. These two HCCs had T1 hyperintense appearance without signal loss on fat suppression, which was attributed to the presence of intratumoural haemorrhage, copper or iron deposits.[16] Two of false-positive non-HCCs were associated with liver iron overload. The presence of iron molecules within the vicinity of the region studied might decrease the role of this imaging technique. This was a well-known situation in which iron deposition in HCCs or in liver tissue (either as haemochromatosis or haemosiderosis) might distort the magnetic field leading to a marked loss of signal and prevent the detection of fat.[16] Because the dual-echo chemical-shift MRI is confounded by T2* bias induced by local field inhomogeneities originating from paramagnetic ions, such as iron, which cause a significant signal drop on in-phase images, and consequently, result in a false underestimating of tissue fat content.[17]

Four patients with metastases had intratumoural fat leading to a misdiagnosis of HCC. This could be related to elevated fatty acid synthesis in tumour tissues such as colon, stomach, breast, ovarian, and lung carcinoma.[38]

The discriminative ability of the fat percentage subtraction score to detect intratumoural fat in patients with or without hepatic steatosis was also analysed. In the present series, only three HCCs were associated with fatty liver. In these cases, the fat percentage subtraction scores were higher than the cut-off value of −0.26 and supported the diagnosis of HCC.

The study has some limitations. First, a single MRI unit from one manufacturer was used, and other scanners were not tested; however, it may be speculated that other high-field scanners are likely to produce the same results. Second, the study population had no equivocal lesion, such as a hepatic adenoma or regenerative nodules, which may contain fat. Third, the number of HCCs associated with steatosis in the background liver was small.

In conclusion, the present results suggest that intralesional fat demonstrated by quantitative chemical-shift MRI may be a potentially powerful imaging biomarker to distinguish HCCs from other malignant liver tumours. It can increase the discriminatory ability of MRI along with other hallmark imaging features; however, the presence of iron molecules within the vicinity of the region studied may decrease the role of technique. Further prospective studies are needed to focus on the value of the fat percentage subtraction score in differentiating HCCs from other hepatic lesions.

Conflicts of interests

The authors declare no conflict of interest.

References

1. Jemal A. Trends in the leading causes of death in the United States, 1970–2002. *JAMA* 2005;**294**(10):1255.
2. Bosch FX, Ribes J, Diaz M, *et al*. Primary liver cancer: worldwide incidence and trends. *Gastroenterol* 2004;**127**(5):S5–16.
3. Van Den Bos IC, Hussain SM, Terkivatan T, *et al*. Stepwise carcinogenesis of hepatocellular carcinoma in the cirrhotic liver: demonstration on serial MRI. *J Magn Reson Imaging* 2006;**24**(5):1071–80.
4. Krinsky GA, Lee VS, Theise ND, *et al*. Hepatocellular carcinoma and dysplastic nodules in patients with cirrhosis: prospective diagnosis with MRI and explantation correlation. *Radiology* 2001;**219**(2):445–54.
5. Hamm B, Thoeni RF, Gould RG, *et al*. Focal liver lesions: characterization with nonenhanced and dynamic contrast material-enhanced MRI. *Radiology* 1994;**190**(2):417–23.
6. Siripongsakun S, Lee JK, Raman SS, *et al*. MRI detection of intratumoural fat in hepatocellular carcinoma: potential biomarker for a more favorable prognosis. *AJR Am J Roentgenol* 2012;**199**(5):1018–25.
7. Salomao M, Remotti H, Vaughan R, *et al*. The steatohepatitic variant of hepatocellular carcinoma and its association with underlying steatohepatitis. *Hum Pathol* 2012;**43**(5):737–46.
8. Purysko AS, Remer EM, Coppa CP, *et al*. LI-RADS: a case-based review of the new categorization of liver findings in patients with end-stage liver disease. *Radiographics* 2012 Nov 1;**32**(7):1977–95.
9. Mitchell DG, Bruix J, Sherman M, *et al*. LI-RADS (liver imaging reporting and Data system): summary, discussion, and consensus of the LI-RADS management working group and future directions. *Hepatology* 2015 Mar 1;**61**(3):1056–65.
10. Mitchell DG, Kim I, Chang TS, *et al*. Fatty liver: chemical shift phase-difference and suppression magnetic resonance imaging techniques in animals, phantoms, and humans. *Invest Radiol* 1991;**26**(12):1041–52.
11. Yu JS, Chung JJ, Kim JH, *et al*. Fat-containing nodules in the cirrhotic liver: chemical-shift MRI features and clinical implications. *AJR Am J Roentgenol* 2007;**188**(4):1009–16.
12. Martin J, Sentis M, Zidan A, *et al*. Fatty metamorphosis of hepatocellular carcinoma: detection with chemical shift gradient-echo MRI. *Radiology* 1995;**195**(1):125–30.
13. Bruix J, Sherman M. Management of hepatocellular carcinoma: an update. *Hepatology* 2011;**53**(3):1020–2.
14. Qayyum A, Goh JS, Kakar S, *et al*. Accuracy of liver fat quantification at MRI: comparison of out-of-phase gradient-echo and fat-saturated fast spin-echo techniques—initial experience. *Radiology* 2005;**237**(2):507–11.
15. Sirlin CB. Invited commentary on Image-based quantification of hepatic fat: methods and clinical applications. *Radiographics* 2009;**29**:1277–80.
16. Curvo-Semedo L, Brito JB, Seco MF, *et al*. The hypointense liver lesion on T2-weighted MR images and what it means. *RadioGraphics* 2010;**30**(1):e38.
17. Virtanen JM, Pudas TK, Ratilainen JA, *et al*. Iron overload: accuracy of in-phase and out-of-phase MRI as a quick method to evaluate liver iron load in haematological malignancies and chronic liver disease. *Br J Radiol* 2012;**85**(1014):e162–7.
18. Ferlay J, Shin HR, Bray F, *et al*. Estimates of worldwide burden of cancer in 2008: GLOBOCAN 2008. *Int J Cancer* 2010;**127**(12):2893–917.
19. Fattovich G, Stroffolini T, Zagni I, *et al*. Hepatocellular carcinoma in cirrhosis: incidence and risk factors. *Gastroenterology* 2004;**127**(5):S35–50.
20. Kudo M. Multistep human hepatocarcinogenesis: correlation of imaging with pathology. *J Gastroenterol* 2009;**44**(S19):112–8.
21. Bialecki ES, Ezenekwe AM, Brunt EM, *et al*. Comparison of liver biopsy and noninvasive methods for diagnosis of hepatocellular carcinoma. *Clin Gastroenterol Hepatol* 2006;**4**(3):361–8.
22. Ronot M, Vilgrain V. Hepatocellular carcinoma: diagnostic criteria by imaging techniques. *Best Pract Res Clin Gastroenterol* 2014;**28**(5):795–812.
23. Asayama Y, Nishie A, Ishigami K, *et al*. Fatty change in moderately and poorly differentiated hepatocellular carcinoma on MRI: a possible mechanism related to decreased arterial flow. *Clin Radiol* 2016;**71**(12):1277–83.
24. Yahagi N, Shimano H, Hasegawa K, *et al*. Co-ordinate activation of lipogenic enzymes in hepatocellular carcinoma. *Eur J Cancer* 2005;**41**(9):1316–22.
25. Sahini N, Borlak J. Recent insights into the molecular pathophysiology of lipid droplet formation in hepatocytes. *Prog Lipid Res* 2014;**54**:86–112.
26. Calvisi DF, Wang C, Ho C, *et al*. Increased lipogenesis, induced by AKT-mTORC1-RPS6 signaling, promotes development of human hepatocellular carcinoma. *Gastroenterology* 2011;**140**(3):1071–83. e5.

27. Yamashita T, Honda M, Takatori H, *et al*. Activation of lipogenic pathway correlates with cell proliferation and poor prognosis in hepatocellular carcinoma. *J Hepatol* 2009;**50**(1):100–10.
28. Björnson E, Mukhopadhyay B, Asplund A, *et al*. Stratification of hepatocellular carcinoma patients based on acetate utilization. *Cell Rep* 2015;**13**(9):2014–26.
29. Pacifico L, Celestre M, Anania C, *et al*. MRI and ultrasound for hepatic fat quantification: relationships to clinical and metabolic characteristics of pediatric nonalcoholic fatty liver disease. *Acta Paediatr* 2007;**96**(4):542–7.
30. Reeder SB, Cruite I, Hamilton G, *et al*. Quantitative assessment of liver fat with magnetic resonance imaging and spectroscopy. *J Magn Reson Imaging* 2011;**34**(4):729–49.
31. Kadoya M, Matsui O, Takashima T, *et al*. Hepatocellular carcinoma: correlation of MRI and histopathologic findings. *Radiology* 1992;**183**(3):819–25.
32. Min JH, Kim YK, Lim S, *et al*. Prediction of microvascular invasion of hepatocellular carcinomas with gadoxetic acid-enhanced MRI: impact of intra-tumoural fat detected on chemical-shift images. *Eur J Radiol* 2015;**84**(6):1036–43.
33. Kutami R, Nakashima Y, Nakashima O, *et al*. Pathomorphologic study on the mechanism of fatty change in small hepatocellular carcinoma of humans. *J Hepatol* 2000;**33**(2):282–9.
34. Noureddin M, Lam J, Peterson MR, *et al*. Utility of magnetic resonance imaging versus histology for quantifying changes in liver fat in nonalcoholic fatty liver disease trials. *Hepatology* 2013;**58**(6):1930–40.
35. Fischer MA, Raptis DA, Montani M, *et al*. Liver fat quantification by dual-echo MRI outperforms traditional histopathological analysis. *Acad Radiol* 2012;**19**(10):1208–14.
36. Chernyak V, Fowler KJ, Kamaya A, *et al*. Liver Imaging-Reporting and Data System (LI-RADS) version 2018: imaging of hepatocellular carcinoma in at-risk patients. *Radiology* 2018;**289**(3):816–30.
37. Choi JY, Lee JM, Sirlin CB. CT and MRI diagnosis and staging of hepatocellular carcinoma: part II. Extracellular agents, hepatobiliary agents, and ancillary imaging features. *Radiology* 2014;**273**(1):30–50.
38. Kuhajda FP. Fatty-acid synthase and human cancer: new perspectives on its role in tumour biology. *Nutrition* 2000;**16**(3):202–8.